foods

MDPI

Article

Two-Phase Extraction Processes, Physicochemical Characteristics, and Autoxidation Inhibition of the Essential Oil Nanoemulsion of *Citrus reticulata* Blanco (Tangerine) Leaves

Marwan M. A. Rashed [1,2,*], Ling You [1], Abduljalil D. S. Ghaleb [3] and Yonghua Du [1]

[1] Key Laboratory of Fermentation Resource and Application in Sichuan Higher Education, Faculty of Agriculture, Forestry and Food Engineering, Yibin University, Yibin 644001, China
[2] School of Biological and Food Engineering, Suzhou University, Bianhe Middle Road 49, Yongqiao, Suzhou 234000, China
[3] Faculty of Applied and Medical Science, AL-Razi University, Al-Rebatt St., Sana'a 216923, Yemen
* Correspondence: marwanrashed6@ahszu.edu.cn

Abstract: Combined ultrasound–microwave techniques and pre-enzymatic treatment (hemicellulase and cellulase) enhance essential oil isolation from *Citrus reticulata* Blanco (tangerine) leaves (CrBL). Subsequently, synergistic effects of modified amorphous octenyl succinic anhydride starch (OSA-MS), almond oil, and high-energy microfluidics were studied in synergy with ultrasound techniques in the production of CrBL essential oil (CrBL-EO) nanoemulsion (CrBL-EONE). GC–MS was used to study the extraction technique. Dynamic light scattering (DLS) analysis was used with confocal laser scanning microscopy (CLSM) techniques to investigate the nanoemulsion matrices' physical and chemical properties. The D-limonene nanoemulsion (D-LNE) reached the optimal size of droplets (65.3 ± 1.1 r.nm), polydispersity index (PDI) (0.167 ± 0.015), and ζ-potential (−41.0 ± 0.4 mV). Besides, the CrBL-EONE obtained the optimal size of droplets (86.5 ± 0.5 r.nm), PDI (0.182 ± 0.012), and ζ-potential (−40.4 ± 0.8 mV). All the nanoparticle treatments showed significant values in terms of the creaming index (CI%) and inhibition activity (IA%) in the β-carotene/linoleate system with a low degradation rate (DR). The current study's findings showed that integrated ultrasound–microwave techniques and pre-enzymatic treatment could enhance the extraction efficiency of the CrBL-EO. In addition, OSA-MS and almond oil can also be employed to produce CrBL-EONE and D-LNE.

Keywords: *Citrus reticulata* Blanco; two-phase extraction processes; essential oil nanoemulsion; autoxidation inhibition; antioxidant activity; physicochemical characteristics; creaming index

Citation: Rashed, M.M.A.; You, L.; Ghaleb, A.D.S.; Du, Y. Two-Phase Extraction Processes, Physicochemical Characteristics, and Autoxidation Inhibition of the Essential Oil Nanoemulsion of *Citrus reticulata* Blanco (Tangerine) Leaves. *Foods* **2023**, *12*, 57. https://doi.org/10.3390/foods12010057

Academic Editor: Diana De Santis

Received: 3 November 2022
Revised: 6 December 2022
Accepted: 19 December 2022
Published: 22 December 2022

1. Introduction

The consumers' demand for food products with high nutritional value and health safety is increasing, especially with the increasing development in global trade, particularly in the food product sectors. Such emerging trends have led the industry and trade sectors to rethink the selection of food additives and rationalize their use, as well as to the gradual shift in replacing synthetic additives with natural alternatives [1].

Since ancient times, plant-based natural products have been a substantial source of several food additives and pharmaceutical products. Bioactive phytochemicals and plant-based sources can be isolated from flowers (e.g., *Zanthoxylum schinifolium* [2]), leaves (e.g., *Lavandula pubescens* [3]), fruit (e.g., *Solanum lycocarpum* St. Hil. (Solanaceae) [4]), stems (e.g., *Warburgia ugandensis* [5]), and roots (e.g., ginger [6]). Most phytochemicals found in plant-based sources fall into the following biochemical categories: polyphenols, terpenes, alkaloids, and glycosides [7]. Bioactive compounds, particularly those that form the chemical composition of essential oils, have attracted great interest from researchers and producers alike due to the diversity of their biological activities.

Medicinal plant use is widespread worldwide because of their distinctive chemical components that provide several desired bioactive properties. Since ancient times, traditional medicine therapists have used essential oils to prevent, avoid, or treat several diseases and provide the health benefits required. With the development of scientific research and the technological revolution in various aspects, essential oils have become very important due to their chemical composition that is rich in biologically active compounds and their importance in the production of healthy and nutritious products [8], processed foods [9,10], the pharmaceutical industry [11–13], cosmetics [14–16], anxiety reduction [17], and fragrance applications [18], either directly or indirectly.

The *Citrus* genus is an essential member of the Rutaceae family and includes tangerines, oranges, lemons, calamansi, limes, kumquats, mandarins, pomelos, and grapefruits. *Citrus reticulata* Blanco (tangerine) is one of the most significant members of the *Citrus* genus, and its essential oil has high health and economic benefits [19]. *Citrus* essential oils are widely used as an additive in food products, either to add a distinctive flavor [20] or to extend the shelf life of food products for a longer period due to their bioactive properties, such as antioxidant and antimicrobial action [21,22]. However, using essential oils as a replacement for synthetic additives is still in the early phase due to concerns about the chemical composition of some essential oils that are still being researched and their safety being investigated. Some of these concerns and limitations are, but not limited to, the safety of the chemical composition and effective concentration of the essential oil. In addition to the possibility of using essential oils in nanosystems, which has proven effective in maintaining the bioactive properties of many types of essential oils, the costs and benefits of applying EOs and nanotechnology in the field of food processing are also of interest [8].

Several modern techniques have been employed together with traditional extraction techniques to extract essential oils from aromatic plants. Some of these techniques have proven successful, and others are still being tested. The successful extraction techniques include liquid–liquid extraction, dispersed liquid–liquid microextraction, solid-phase extraction, solid-phase microextraction, ultrasound-assisted extraction, and microwave-assisted extraction [23].

Studies investigating the possibility of employing nanoemulsions as an emerging technology still attract many scholars in the food industry's research and development sector. The success of a nanosystem is based on the production of an optimal nanoemulsion that meets the desired functional properties to increase the stability of the essential oil's components against oxidation as well as its aqueous phase solubility and maintain its aromatic properties [2,24]. Despite the lipophilic properties of essential oils, they vary greatly in their chemical composition, making it necessary to carefully select the type of wall material in nanosystems to obtain highly stable nanoemulsions. For instance, the dominant components of rose oils are alcohol monoterpenes with a concentration of more than 70%, and citronellol is the major component [25]. In contrast, the dominant component of *Citrus* essential oils in general, and of the *C. reticulata* Blanco (tangerine) leaf essential oil in particular (the essential oil under study), is a linear monoterpene with a concentration of more than 90%, and D-limonene is the major component. Similarly to other essential oils, tangerine oil has low chemical stability and poor solubility in water [26]. Modified amorphous octenyl succinic anhydride starch (OSA-MS) is one of the most commonly used polysaccharides as a wall material in the preparation of nanoemulsions due to its distinctive chemical structure consisting of an amphipathic molecule with hydrophobic octenyl succinate groups and hydrophilic and hydroxyl groups of native starch. Still, the success and effectiveness of OSA-MS use are governed by the compatibility between the chemical composition of OSA-MS with the chemical composition of the core materials, the biologically active substances [25,27].

The current study focused on using the extracted essential oil from *C. reticulata* Blanco (tangerine) leaves using ultrasound–microwave techniques and pre-enzymatic treatment to enhance a novel form of nanoemulsion. The innovative technique can improve the physicochemical properties (ζ-potential, polydispersity index, and droplet size distribution)

of nanoemulsion-based *C. reticulata* Blanco essential oils (CrBL-EO) using almond oil as a carrier substance and OSA-MS as a biodegradable emulsifying agent and wall material.

2. Materials and Methods

2.1. Plant Specimen and Chemicals

Fresh tangerine (*C. reticulata* Blanco) leaves (CrBL) were obtained from a local market in Suzhou City (Suzhou, Anhui, China). Hemicellulase and cellulase from *Aspergillus niger*, β-carotene ($\geq$95%), and Trolox were purchased from Sigma-Aldrich (Darmstadt, Germany). Linoleic acid (85%), 2,2′-azino-bis(3-ethylbenzothiazoline-6-sulfonic acid) (ABTS), 2,2-diphenyl-1-picrylhydrazyl (DPPH), *tert*-butylhydroquinone (TBHQ), and 2,6-bis(1,1-dimethylethyl)-4-methylphenol (BHT) were purchased from TCI EUROPE N.V. (Brussels, Belgium). Modified amorphous octenyl succinic anhydride starch (OSA-MS) Hi-cap 100 was purchased from National Starch and Chemical Co. (Bridgewater, NJ, USA). Tween-40 and Tween-80 were procured from Sinopharm Chemical Reagent Co. Ltd. (Shanghai, China). Deionized distilled water used to prepare the nanoemulsion was produced using a Milli-Q water purification system (Millipore Corp., Darmstadt, Germany). Dyes nile red and fluorescein isothiocyanate (FITC) were purchased from Sigma-Aldrich Co. (Deisenhofen, Germany). All the other reagents used were of analytical grade.

2.2. Preparation of Tangerine Leaves

Tangerine leaves (CrBL) were soaked in an aqueous NaCl solution (1%, w/v), then washed with running tap water and gently dried at 40 $\pm$ 1 °C in an air oven (DHG-9245A, Shanghai Yiheng Scientific Instrument Co., Ltd., Shanghai, China) for 72 h. Then, the dried leaves were ground using a high-speed grinder to obtain a fairly fine powder. The fine powder sample (CrBL.P) was kept at 4 $\pm$ 1 °C in polyethylene bags protected from light until the next step. The moisture content of the CrBL.P was measured to be 6.5%.

2.3. Two-Phase Pre-Extraction of CrBL Essential Oil (CrBL-EO)

Two-phase extraction processes using pre-enzymolysis (first phase) followed by pre-ultrasound homogenizer-assisted extraction using a JY98-III DN Ultrasound Homogenizer, FeiQi Industry & Trade Co., Ltd. (Nanjing, China) (second phase), were performed. According to our previous study [23], with a slight modification, each fine powder sample of CrBL.P (100 g) was added to 500 mL of deionized distilled water that contained a mixture of 20 mg cellulase/hemicellulase at a ratio of 1:1 (w/w). The treatments were kept at 42 $\pm$ 1 °C for two h using a shaking water bath. All the treatments were subjected to the pre-ultrasound homogenizer-assisted phase. The ultrasound power and frequency of the pre-ultrasound homogenizer-assisted extraction were set at 150 W and 20 kHz. The total time programmed for the sonication treatment was 12 min, and the mixture was exposed to ultrasound waves for 5 min. The processing temperature (40 $\pm$ 2 °C) was continuously controlled using an external thermostatic cold-water bath. Each treatment was divided into two equal parts. Each treatment (in its two parts) was subjected to hydrodistillation for 30 min (for the first part) and 180 min (for the second part) using a Clevenger-type apparatus to isolate CrBL-EO. The hydrodistillation temperature was set at 100 $\pm$ 2 °C. [28]. The CrBL-EO samples obtained from each treatment were collected, weighed, and dried using anhydrous sodium sulphate. The collected samples were stored at 0 °C in brownish, airtight, and sealed vials. The treatments were coded as shown in Table 1.

Table 1. Codes for the treatments subject to essential oil extraction.

Sample	Isolation Time	Code
CrBL.P without treatment (control)	30 min 180 min	CrBL-EO_{C1} CrBL-EO_{C2}
CrBL.P with pre-enzymolysis treatment	30 min 180 min	CrBL-EO_{E1} CrBL-EO_{E2}
CrBL.P with ultrasound–microwave treatment	30 min 180 min	CrBL-EO_{US1} CrBL-EO_{US2}
CrBL.P with pre-enzymolysis and ultrasound–microwave treatment	30 min 180 min	CrBL-EO_{EUS1} CrBL-EO_{EUS2}

The CrBL-EO yields (%) and the increase rates (IR) of the EOs were calculated according to Equations (1) and (2):

$$\text{CrBL} - \text{EO } \textit{Yield}\% = \left[\frac{\text{EO obtained (g)}}{\text{Initial wt. of CrBL powder (g)}}\right] \times 100 \quad (1)$$

$$\text{IR}\% = \left[\left(\frac{A1}{A0}\right) \times 100\right] - 100 \quad (2)$$

where IR% is the increase rate, $A1$ is the EO obtained from a CrBL treatment, and $A0$ is the EO obtained from the control treatment (CrBL-EOc).

The separated CrBL-EO samples were kept in sealed brown glass vials at 4 °C until the next analysis.

2.4. Gas Chromatography–Mass Spectrometry (GC–MS) Analysis

The CrBL-EO treatments were analyzed to investigate the volatile compounds using an Agilent GC–MS system equipped with a gas chromatograph (7890A) and a mass spectrometer detector (5975C). The GC was fitted with an HP-5MS column (30 m × 0.25 mm internal diameter and 0.25 µm film thickness, J&W Scientific, Folsom, CA, USA) to separate the volatile compounds. Helium served as a carrier gas at a 1 mL/min flow rate with a 10:1 split ratio and a splitless injection volume of 1 µL. The gradient temperature was programmed as follows: 40 °C for 1 min, rising to 150 °C at 4 °C/min and maintained for 6 min; rising at 4 °C/min to 210 °C and maintained for 1 min. The injector and the detector were kept at 280 °C and 220 °C, respectively. For mass spectrometry (MS), electron ionization (EI) with an ionization energy voltage of 70 eV, emission current of 35 mA, and a spectral zone of 40–550 m/z was performed. The National Institute of Standards and Technology (NIST) 08, 2005 Library (Gaithersburg, MD, USA), Wiley 7 Library (Wiley, New York, NY, USA), and published mass spectra were used to identify the essential oil components based on their MS data.

2.5. Microstructure Observation Using Scanning Electron Microscopy (SEM)

The treatments (CrBL-EO_{C2}, CrBL-EO_{E2}, CrBL-EO_{US2}, and CrBL-EO_{EUS2}) were scanned using a SEM SU 1510 from Hitachi High-Technologies Corp. (Tokyo, Japan) to study the effect of two-phase extraction on the microstructure of CrBL.P leaf cells. All the prepared samples were fixed onto the sample holder using aluminum tape. The fixed samples were sputtered with a thin layer of gold and palladium using an ionic sputter coater. High vacuum conditions at an accelerating beam voltage of 5 kV were used. The working distance was set at 12.5 mm with a magnification coefficient of 1200×.

2.6. Measurement of Anti-Free Radical Activities

2.6.1. DPPH• Scavenging Activity Assay

Free radical scavenging activities of the CrBL-EO treatments were assessed as described previously [29] with a slight modification: 100 µL of each working sample at the

final concentration of 0.2 mg/mL were mixed with 3 mL DPPH solution. The DPPH$^{\bullet}$ scavenging activity (DPPH$^{\bullet}$-SA%) was calculated as follows:

$$\text{DPPH}^{\bullet}\text{-SA\%} = \left[\frac{OD_0 - OD_1}{OD_0}\right] \times 100 \quad (3)$$

where OD_0 and OD_1 mean the optical density of the control sample and a targeted CrB-EO treatment.

2.6.2. ABTS$^{\bullet+}$ Scavenging Activity (ABTS$^{\bullet+}$-SA) Assay

The ABTS$^{\bullet+}$-SA assay was performed according to Rashed et al. [23] with a slight modification: 100 µL of each working sample at the final concentration of 0.2 mg/mL were mixed with 3 mL ABTS solution. The calibration curve of Trolox was used to explain the free radical scavenging activity of the CrBL-EO treatments in mM Trolox.

Given that the CrBL-EO$_{EUS2}$ treatment demonstrated the best yield (%), DPPH$^{\bullet}$-SE (%), and ABTS$^{\bullet+}$-SA (mM Trolox), it was selected for the rest of the subsequent analyses.

D-limonene, TBHQ, and BHT (100 µL each) were used as the positive samples, all at the same concentration (0.2 mg/mL).

2.7. Preparation of the CrBL-EO$_{EUS2}$ Nanoemulsion

Nanoemulsions were produced in two phases: aqueous and organic. Exactly 3 g OSA-MS was dissolved with 92 mL deionized distilled water at 25 + 1 °C to prepare the aqueous phase. The solution was subjected to magnetic stirring overnight to ensure full hydration. The organic phase included 1.5 g almond oil, 2.5 g CrBL-EO$_{EUS2}$, and 1 g Tween-80 (a nonionic surfactant). For full homogenization, the organic phase was subjected to magnetic stirring at 40 °C for 15 min and then at room temperature for 45 min (CrBL-EONE). A control sample (CNE) was prepared without adding CrBL-EO$_{EUS2}$. A comparison sample was prepared using D-limonene (D-LNE) instead of CrBL-EO$_{EUS2}$. Coarse emulsions were prepared by adding the organic phase drop-by-drop to the aqueous phase during the homogenization process at 18,000 rpm for 5 min using a high-speed homogenizer (Ultra Turrax T25 Basic, IKA, Staufen, Germany). The working treatments were then subjected to the pulsed sonication process at an ultrasound power of 960 W and the total sonication time of 2 s working time followed by 3 s elapsed time (total time of 15 min). All the nanoemulsions were subjected to further homogenization by passing through a high-pressure homogenizer at 100 MPa for five cycles using high-pressure homogenizer ATS AH2100 (ATS Engineering Inc., Brampton, ON, Canada). All the produced nanoemulsions were used in the subsequent analyses.

2.8. Physicochemical Characterization of the Nanoemulsion Treatments

The physicochemical properties of the CNE, CrBL-EONE, and D-LNE nanoemulsions were analyzed using a Zetasizer Nano (ZS, Malvern Instrument Ltd., Worcestershire, UK) based on the dynamic light scattering theory (DLS). The physicochemical assessment included the following measurements: *Z*-average in radius nanometers (r.nm), PDI of the size distribution, and ζ-potential. Each working sample (100 µL) was diluted 100× using deionized distilled water before analysis. All the measurements were performed at 25 °C in triplicate.

2.9. Creaming Index (CI%)

According to Rashed et al. [27], the creaming index (CI%) measurement was employed to evaluate the stability of the nanoemulsions prepared under storage at 25 °C for 30 days. The CI% was calculated as a percentage according to Equation (4):

$$\text{CI\%} = \frac{TH_{NEL}}{TH_{SL}} \quad (4)$$

where TH_{NEL} refers to the visual observation of the total initial layer height of the nanoemulsion, and TH_{SL} is the separated serum layer height.

2.10. Confocal Laser Scanning Microscopy (CLSM)

The morphological investigation of the formulated nanoemulsions was conducted using a Zeiss Laser Scanning Microscopy 710 microscope (Zeiss Inc., Braunschweig, Germany) [30,31].

2.11. Thermal Autoxidation Using Inhibition of the β-Carotene/Linoleate System

Autoxidation inhibition of the CrBL-EO_{EUS2}, D-limonene, CrBL-EONE, D-LNE, and TBHQ treatments was determined in the β-carotene/linoleic acid coupled system according to Rashed et al. [3] with a slight modification. To prepare the β-carotene/linoleate emulsion (β-CLE), 0.2 mg β-carotene was dissolved in 10 mL chloroform. Two mL of the β-CL solution were added into a round-bottom rotary flask with 20 mg linoleic acid and 200 mg Tween-40. After evaporating the chloroform using a rotary evaporator at 35 °C, 50 mL deionized distilled water (HPLC grade) was added to the reaction flask. The reaction substances were homogenized with manual shaking to obtain β-CLE. Five mL of β-CLE were pipetted into test tubes containing 0.2 mL (200 mgL^{-1}) of the CrBL-EO_{EUS2}, CrBL-EONE, or D-LNE treatments. In addition, 0.2 mL (200 mg/L) of standard TBHQ or D-limonene were used as the comparison samples. The control treatment consisted of 0.2 mL methanol instead of the extract. The zero-time absorbance was read at 470 r.nm once the emulsion was added to each test tube. All the samples were exposed to thermal autoxidation at 50 °C using a shaking water bath. Absorbance measurements were recorded every 20 min for 60 min. The disappearance of the β-carotene color in the control treatment indicates the end of the incubation time. All the treatments were analyzed in triplicate. The degradation rate (DR) of all the samples was calculated according to zero-order kinetic interactions according to the following Equation (5):

$$\mathrm{DR} = \frac{\ln\left(\frac{a}{b}\right)}{\frac{1}{60}} \quad (5)$$

where ln is the natural logarithm, a is the measured absorbance value at the zero time, and b refers to the measured absorbance value at the final time of treatment (60 min).

The percentage of the inhibition activity (IA%) was calculated as the inhibition ability of the CrBL-EO_{EUS2} treatment compared with the inhibition ability of the control sample according to the following Equation (6):

$$\mathrm{IA\%} = \left[\frac{DR_0 - DR_1}{DR_0}\right] \times 100 \quad (6)$$

where DR_0 is the deterioration rate of the control treatment and DR_1 is the target treatment's (CrBL-EO_{EUS2}, CrBL-EONE, D-LNE, TBHQ, and D-limonene) deterioration rate.

The differences between the IA% values at 20 min and 60 min (ΔIA%) were calculated (Equation (7)) to determine the stability of the emulsions during thermal treatment for 60 min.

$$\Delta\mathrm{IA\%} = \mathrm{IA\%_{20min}} - \mathrm{IA\%_{60min}} \quad (7)$$

2.12. Statistical Analysis

The data were expressed as the means ± standard deviation using SPSS 25.0 (SPSS Inc., Chicago, IL, USA). One-way analysis of variance (ANOVA) according to Duncan's new multiple-range test was used to analyze the significant differences between the means. The differences were considered significant at $p < 0.05$.

3. Results

3.1. Two-Phase Extraction of CrBL-EO

Table 2 shows the yield (%) obtained for all the CrBL-EO treatments and the increase rate (IR%) between the 30 min hydrodistillation and the 180 min hydrodistillation. The

yield (%) values from the highest to the lowest were as follows: 1.03, 0.9, 0.86, 0.86, 0.81, 0.8, 0.72, and 0.65% for CrBL-EO_{EUS2}, CrBL-EO_{EUS1}, CrBL-EO_{US2}, CrBL-EO_{E2}, CrBL-EO_{US1}, CrBL-EO_{E1}, CrBL-EO_{C2}, and CrBL-EO_{C1}, respectively. The yields of extracted essential oils are generally affected by several factors, the most important of which are origin, season, environmental factors, maturity stage (immature, semi-ripe, or mature), isolation technique, and isolation time [32,33]. Several studies focused on isolating the essential oil from *C. reticulata* Blanco (tangerine) waste. Hydrodistillation of *Citrus* peel from four *Citrus* species (*Citrus aurantifolia* (lime), *Citrus limon* (lemon), *Citrus limetta* (sweet lime), and *Citrus reticulata* (mandarin)) yielded an essential oil in the range of 0.48–0.75% after 4–5 h of hydrodistillation [34]. The present study obtained higher yield values (%) for *C. reticulata* Blanco (tangerine) leaves, with the maximum yield (%) of 1.03 ± 0.06 for the CrBL-EO_{EUS2} treatment; the lowest yield (%) was 0.65 ± 0.02 for the CrBL-EO_{C1} treatment. The isolation time during the hydrodistillation process significantly affected the yield increase (YI%) for all the treatments, with a YI% of 14.5% between the CrBL-EO_{EUS1} and CrBL-EOE_{US2} treatments, 11.86% between the CrBL-EO_{C1} and CrBL-EO_{C2} treatments, 7.47% between the CrBL-EO_{E2} and CrBL-EO_{US1} treatments, and 7.07% between the CrBL-EO_{US2} and CrBL-EO_{EUS1} treatments. The importance of enzymatic treatment is in its ability to dismantle the cellular structure of the cell wall in the plant tissue and depolymerize the polysaccharides of plant cell walls [23,35–39]. Hence, it would significantly increase the effectiveness of the subsequent ultrasound–microwave integrated treatment [29], thus enhancing the qualitative and quantitative (excluding yield%) quality of isolated CrBL-EO. Literature also reports that the cellulase achieved the highest yield of oil release from pumpkin seeds compared with the control sample using a microwave-assisted aqueous enzymatic extraction technique [40,41]. In general, these results illustrate that the mixture of hydrolysis enzymes (cellulase/hemicellulase) combined with ultrasound–microwave integrated treatment could enhance the release of the EO extracted from CrBL.P (CrBL-EO).

Table 2. Chemical composition of the CrBL-EO treatments.

RT [1]	Components	Concentration (%)							
		C_{30}	C_{180}	E_{30}	E_{180}	US_{30}	US_{180}	EUS_{30}	EUS_{180}
01.352	Pentane	nd [2]	2.00	nd	nd	nd	2.32	nd	nd
01.603	2-methylpentane	21.61	18.8	21.63	20.13	21.24	26.49	18.7	20.46
02.133	Cyclohexane	1.56	1.69	1.53	1.46	1.54	2.02	1.4	1.5
07.455	(−)-α-pinene	1.59	1.17	1.66	1.6	1.56	1.18	1.35	1.14
09.448	(−)-β-pinene	4.1	2.78	3.93	3.96	3.99	2.64	3.05	3.11
09.472	β-phellandrene	nd	tr [3]	0.65	tr	0.84	tr	nd	tr
10.952	D-limonene	59.35	50.32	58.74	54.14	57.2	52.44	65.7	56.68
13.307	Linalool	0.94	tr	0.75	tr	1.05	tr	0.55	tr
14.857	β-terpineol	tr	tr	tr	0.55	tr	tr	tr	0.61
16.023	Terpinen-4-ol	1.76	1.19	1.14	1.08	1.29	0.97	1.25	1.02
16.530	α-terpineol	0.92	1.83	1.2	1.99	1.2	1.5	1.25	2.83
17.095	Decanal	0.83	0.62	0.99	0.8	1.29	0.78	0.75	0.91
17.900	β-citronellol	0.69	0.58	0.56	tr	0.71	0.5	0.75	0.62
19.392	dl-perillaldehyde	0.83	0.75	0.56	tr	0.61	0.5	0.85	0.79
19.998	*p*-mentha-1(7),8(10)-dien-9-ol	tr	tr	tr	tr	tr	nd	tr	0.87
20.785	2-methoxy-4-vinylphenol	nd	nd	nd	0.75	nd	nd	nd	0.35
23.373	(-)-cis-β-elemene	tr	tr	tr	0.56	tr	0.53	0.55	0.64
23.932	Dodecanal	tr	0.54	tr	0.72	tr	0.56	tr	0.83
26.159	(-)-germacrene D	tr	tr	tr	0.51	tr	tr	tr	0.62
31.836	Longifolene	nd	tr	nd	0.61	nd	nd	nd	0.5
36.592	α-sinensal	tr	1.87	0.55	1.84	tr	1.23	1.5	2.26
44.286	*n*-hexadecanoic acid	tr	2.28	tr	1.17	tr	0.53	tr	1.53
48.821	Linoleic acid	tr	0.72	tr	1.07	nd	nd	nd	nd
	Yield % Total	0.65 ± 0.02 [f]	0.72 ± 0.03 [e]	0.80 ± 0.02 [d]	0.86 ± 0.02 [c]	0.81 ± 0.03 [d]	0.86 ± 0.02 [c]	0.90 ± 0.02 [b]	1.03 ± 0.06 [a]
	[4] YI%	–	11.86	–	7.47	–	7.07	–	14.5

[1] Retention time; [2] nd = not detected; [3] tr = trace; [4] YI—yield increase (%). Treatments with the means followed by the same superscripts in the columns did not differ significantly ($p < 0.05$).

3.2. Chemical Composition of the CrBL-EO Treatments

Over 50 volatile components were identified in the CrBL-EO treatments. Table 2 shows the 23 volatile components at a concentration ≥ 0.5%. D-limonene was the main component of the CrBL-EO chemical composition in all the treatments. The concentrations (%) of D-limonene were as follows: 65.7, 59.35, 58.74, 57.2, 56.68, 54.14, 52.44, and 50.32% for EUS_{30} (CrBL-EO_{EUS1}), C_{30} (CrBL-EO_{C1}), E_{30} (CrBL-EO_{E1}), US_{30} (CrBL-EO_{US1}), EUS_{180} (CrBL-EO_{EUS1}), E_{180} (CrBL-EO_{E2}), US_{180} (CrBL-EO_{US2}), and C_{180} (CrBL-EO_{C2}), respectively.

The results show that long-term hydrodistillation negatively affected the concentration of D-limonene in all the CrBL-EO treatments. According to its chemical properties, D-limonene is a natural cyclic monoterpene sensitive to exposure to high temperatures and light [33]. The chemical composition of a broad spectrum of essential oils isolated from most *Citrus* peels or leaves contains D-limonene [19,42]. Treatments with low processing time are compatible with two-phase extraction processes with high efficiency in enhancing the qualitative (antioxidant activity) and quantitative parameters (D-limonene%) of CrBL-EO treatments. This is because high-temperature treatment for a long time can lead to cracking the chemical composition of many of the main components of the EO, especially D-limonene [33]. Based on the literature, the results of this study appear to be consistent with the previously reported data [19].

C_{30} (CrBL-EO_{C1}) and C_{180} (CrBL-EO_{C2}) were the control treatments after 30 and 180 min of incubation time, respectively; E_{30} (CrBL-EO_{E1}) and E_{180} (CrBL-EO_{E2}) were the pre-enzymolysis treatments after 30 and 180 min of incubation time, respectively; US_{30} (CrBL-EO_{US1}) and US_{180} (CrBL-EO_{US2}) were the ultrasound–microwave treatments after 30 and 180 min of incubation time, respectively; EUS_{30} (CrBL-EO_{EUS1}) and EUS_{180} (CrBL-EO_{EUS1}) were the pre-enzymolysis and ultrasound–microwave treatments after 30 and 180 min of incubation time, respectively.

3.3. Microstructure Observation

The microstructure observation of the CrBL-EO_{C2} sample surface demonstrated slight ruptures with partial destruction after isolation of CrBL-EO without using any enzymatic or ultrasound–microwave treatments (Figure 1a) compared to the microstructure of CrBL-EO_{E2} (Figure 1b), CrBL-EO_{US2} (Figure 1c), and CrBL-EO_{EUS2} (Figure 1d). However, significant morphological and structural changes were observed in an enzymatic treatment (CrBL-EO_{E2}), where most glandular structures were ruptured. These findings demonstrate that the destruction of cell walls when using hydrolysis enzymes such as cellulase and hemicellulase occurred and enhanced the release of CrBL-EO from the oily glands of plant cells. This might be attributed to the ability of cellulase and hemicellulase to decompose and hydrolyze the cellulose and hemicellulose layers in plant cell walls [38,43]. In the same context, the ultrasound–microwave treatments of CrBL-EO altered the surface microstructure of CrBL.P, as clearly demonstrated in Figure 1c,d. This effect can be attributed to the cavitation phenomenon resulting from ultrasound power combined with microwave radiation [44]. Therefore, the importance of employing a combination of hydrolysis enzymes (cellulase and hemicellulase) comes from the need to decompose the cell wall's physical barrier to reach the storage glands of volatile and biologically active components and thus enhance the effectiveness of the ultrasound–microwave extraction which ultimately facilitates the access of the solvent into the glandular structures and secretory cavities [29,45].

3.4. Anti-Free Radical Activities

3.4.1. DPPH• Scavenging Activity (DPPH•-SA%)

The anti-free radical activity of the CrBL-EO treatments was measured using an in vitro DPPH• assay. Table 3 shows the values of DPPH•-SA% of CrBL-EO_{C1}, CrBL-EO_{C2}, CrBL-EOE1, CrBL-EO_{E2}, CrBL-EO_{US1}, CrBL-EO_{US2}, CrBL-EO_{EUS1}, and CrBL-EO_{EUS2}, D-limonene, TBHQ, and BHT. TBHQ (91.67%) and D-limonene (90.73%) had the highest value of DPPH•-SA%, with no significant differences, followed by CrBL-EO_{EUS2} (87.5%), CrBL-EONE (87.47%), CrBL-EO_{EUS1} (87.4%), BHT (85.97%), CrBL-EO_{E2} (82.93%), CrBL-EO_{US2} (82.83%), CrBL-EO_{US1} (82.8%), CrBL-EO_{E1} (82.7%), CrBL-EO_{C2} (81.37%), and CrBL-EO_{C1} (80.7%).

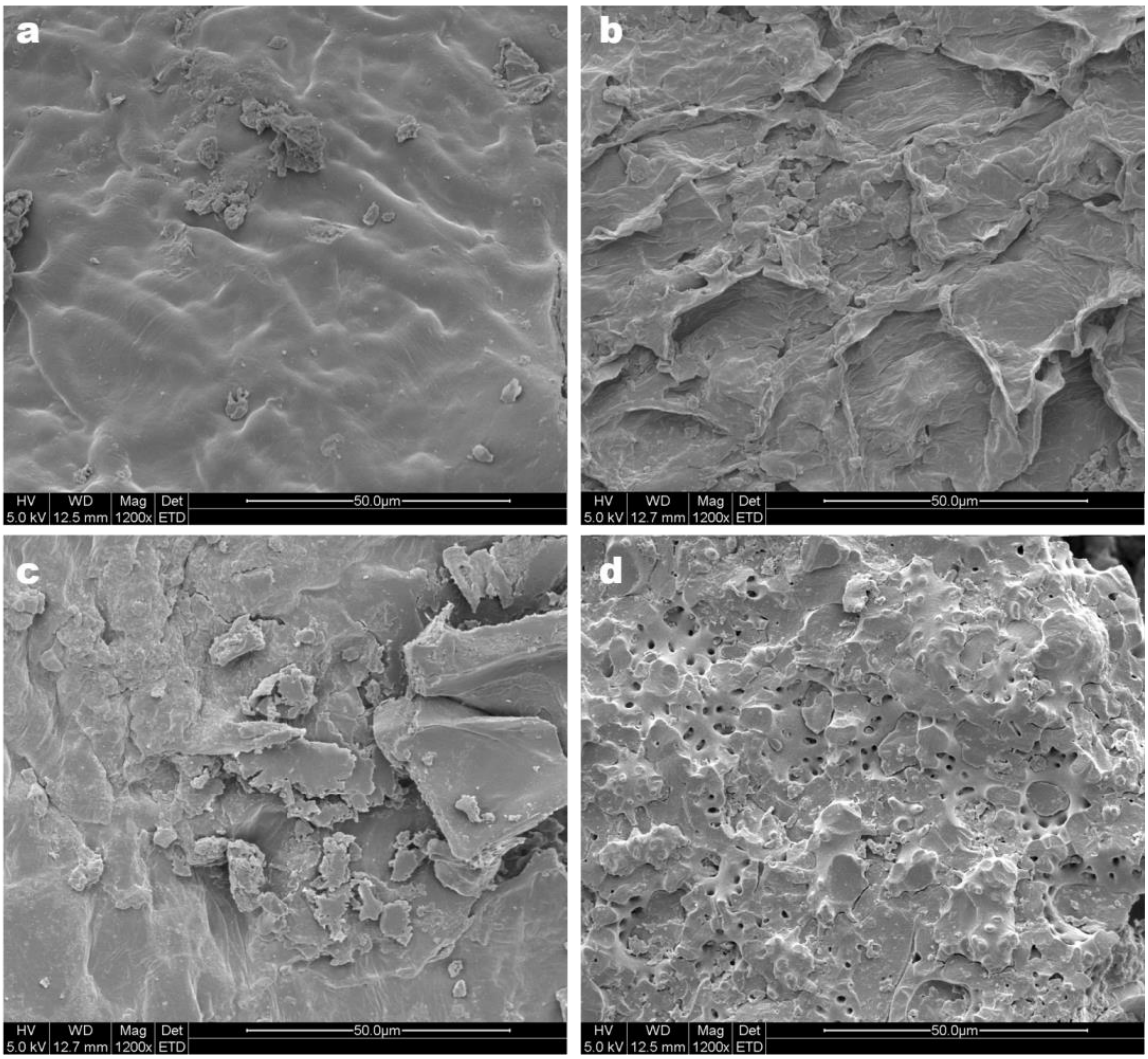

Figure 1. SEM observation of (**a**) the control treatment (CrBL-EO_{C2}); (**b**) pre-enzymolysis treatment (CrBL-EO_{E2}); (**c**) ultrasound–microwave treatment (CrBL-EO_{US2}c); and (**d**) pre-enzymolysis and ultrasound–microwave treatment (CrBL-EO_{EUS2}).

Table 3. DPPH•-SA (%) and $ABTS^{\bullet+}$-SA (mM Trolox) of the CrBL-EO treatments with IR% compared with the control treatment (CrBL-EO_{C2}).

Treatment System	DPPH•-SA (%)		$ABTS^{\bullet+}$-SA (mM Trolox)	
	Result	IR [1]	Result	IR
CrBL-EO_{C1}	80.70 ± 0.20 [e]	–	0.0173 ± 0.0011 [e]	–
CrBL-EO_{C2}	81.37 ± 0.42 [e]	0.00	0.0183 ± 0.0011 [e]	0.00
CrBL-EO_{E1}	82.70 ± 0.20 [d]	1.64	0.0213 ± 0.0011 [d]	16.36
CrBL-EO_{E2}	82.93 ± 0.15 [d]	1.93	0.0217 ± 0.0011 [d]	18.18
CrBL-EO_{US1}	82.80 ± 0.10 [d]	1.76	0.0210 ± 0.0012 [d]	14.55
CrBL-EO_{US2}	82.83 ± 0.25 [d]	1.80	0.0220 ± 0.0007 [d]	20.00
CrBL-EO_{EUS1}	87.40 ± 0.30 [b]	7.41	0.0280 ± 0.0007 [b]	52.73
CrBL-EO_{EUS2}	87.50 ± 0.30 [b]	7.54	0.0283 ± 0.0008 [b]	54.55

Table 3. *Cont.*

Treatment System	DPPH•-SA (%)		ABTS•+-SA (mM Trolox)	
	Result	IR [1]	Result	IR
CrBL-EONE	87.47 ± 0.32 [b]	7.50	0.0277 ± 0.0004 [b]	50.91
D-limonene	90.73 ± 0.47 [a]	11.51	0.0330 ± 0.0014 [a]	80.00
TBHQ	91.67 ± 0.20 [a]	12.66	0.0360 ± 0.0012 [a]	96.36
BHT	85.97 ± 0.80 [c]	5.65	0.0253 ± 0.0011 [c]	38.18

[1] IR—increase rate (%). The values were expressed as the means ± SD (n = 3). CrBL-EO_{C1} and CrBL-EO_{C2} were the control treatments after 30 and 180 min of incubation time, respectively; CrBL-EO_{E1} and CrBL-EO_{E2} were the pre-enzymolysis treatments after 30 and 180 min of incubation time, respectively; CrBL-EO_{US1} and US_{180} CrBL-EO_{US2} were the ultrasound–microwave treatments after 30 and 180 min of incubation time, respectively; CrBL-EO_{EUS1} and CrBL-EO_{EUS1} were the pre-enzymolysis and ultrasound–microwave treatments after 30 and 180 min of incubation time, respectively. Treatments with the means followed by the same superscripts in the columns did not differ significantly ($p < 0.05$).

The increase rate (IR%) was calculated as a relative ratio attributed to the DPPH•-SA% value of the CrBL-EO_{C2} treatment (81.37%). The IR% values from the highest to lowest were as follows: 12.66, 11.51, 7.54, 7.5, 7.41, 5.65, 1.93, 1.8, 1.76, and 1.64% referring to TBHQ, D-limonene, CrBL-EO_{EUS2}, CrBL-EONE, CrBL-EO_{EUS1}, BHT, CrBL-EO_{E2}, CrBL-EO_{US2}, and CrBL-EO_{US1}, respectively. Among all the CrBL-EO treatments, the CrBL-EO_{EUS2} treatment had the highest DPPH•-SA% value (87.5%).

3.4.2. $ABTS^{\bullet+}$ Scavenging Activity ($ABTS^{\bullet+}$-SA)

As depicted in Table 3, the $ABTS^{\bullet+}$-SA values (mM Trolox) of the CrBL-EO treatments and positive treatments agreed and were highly consistent with the results obtained from the DPPH•-SA measurement. In this context, the $ABTS^{\bullet+}$-SA values (mM Trolox) of TBHQ (0.0360 ± 0.0012) with IR% of 96.36% followed by D-limonene (0.0330 ± 0.0014) with IR% of 80% were the highest among all the treatments. Among the CrBL-EO treatments, the CrBL-EO_{EUS2} treatment had the highest $ABTS^{\bullet+}$-SA value (0.0283 ± 0.0008) with an IR% of 54.55%, followed by CrBL-EO_{EUS1} (0.0280 ± 0.0007, IR% of 52.73) and CrBL-EONE (0.0277 ± 0.0004, IR% = 50.91). The $ABTS^{\bullet+}$-SA values (mM Trolox) of the control samples (CrBL-EO_{C1} and CrBL-EO_{C2}) were 0.0173 ± 0.0011 and 0.0183 ± 0.0011, respectively.

The current study's findings agree with the previous studies that described the ABTS assay (at 730 nm) as based on the generation of blue/green ABTS free radicals ($ABTS^{\bullet+}$) and as the optimal method for application in hydrophilic and lipophilic antioxidant systems. In contrast, DPPH free radicals in a DPPH• organic solution are more suitable for application in hydrophobic systems [46].

3.5. Physicochemical Characterization of the CrBL-EONE Treatments

The frequency curves of the particle size distribution (Z-average) in r.nm, including the oversize, PDI, and ζ-potential (mV) curves of the CNE (control treatment), CrBL-EONE, and D-LNE treatments, are shown in Figure 2. The values of Z-average, PDI, and ζ-potential of the CNE treatment were 151.1 ± 6.0 r.nm, 0.356 ± 0.018, and −40.2 ± 0.6 mV, respectively. The values of Z-average, PDI, and ζ-potential for the CrBL-EONE treatment were 86.5 ± 0.5 r.nm, 0.182 ± 0.012, and –40.4 ± 0.8 mV, respectively. The values of the same parameters (Z-average, PDI, and ζ-potential) obtained by the D-LNE treatment were as follows: 65.3 ± 1.1 r.nm, 0.167 ± 0.015, and −41.0 ± 0.4, respectively. Several studies reported that droplet size, polydispersity index, and ζ-potential are among the most traceable physicochemical properties in colloidal systems to measure the stability of nanoemulsions and the integration of their components with high efficiency [8]. The obtained results demonstrated that the produced nanoemulsion-based CrBL-EO, almond oil as the carrier material, OSA-MS as the wall, and Tween-80 as the emulsification agent in synergy with the technique used to prepare the nanoemulsions all contributed to the production of nano-sized particles with homogeneous distribution in the nanoemulsion [27,47].

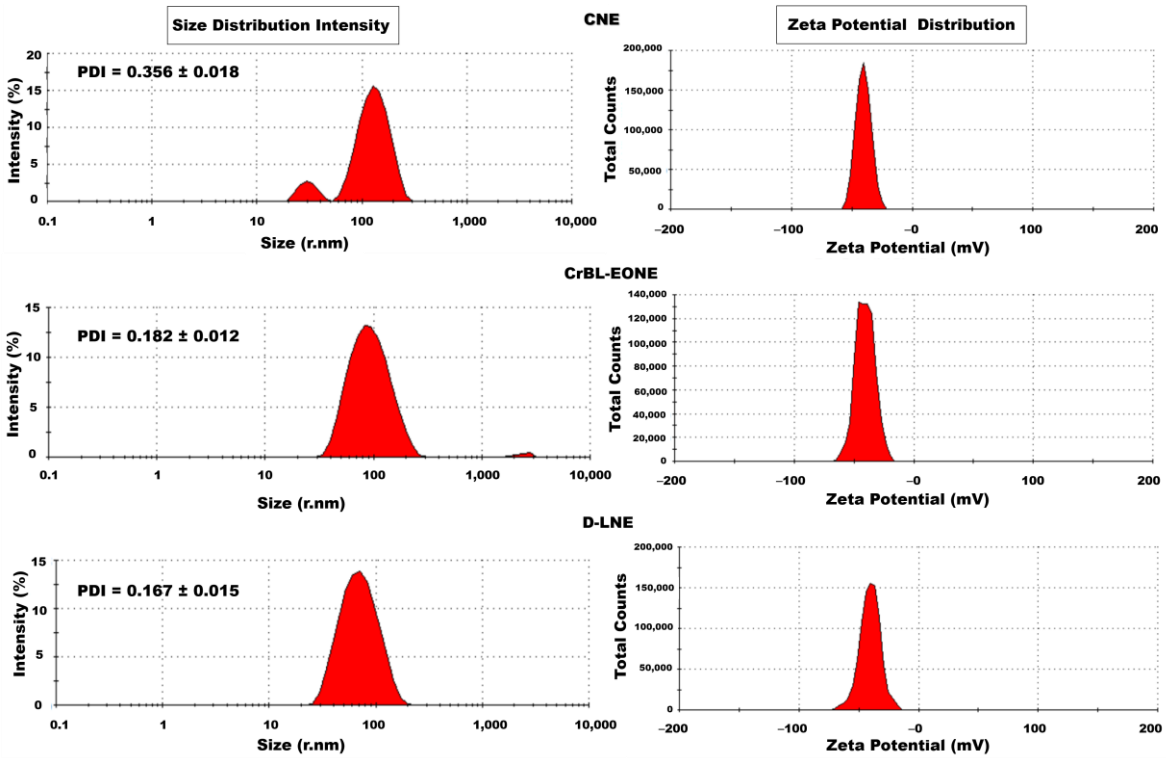

Figure 2. The frequency curves for *Z*-average include the oversize (logarithmic scale), PDI, and ζ-potential values of the control nanoemulsion treatment (CNE), *C. reticulata* leaf essential oil nanoemulsion (CrBL-EONE), and D-limonene nanoemulsion (D-LNE) (linear scale).

3.6. Creaming Index (CI%)

Figure 3 shows the creaming index (CI%) values of the nanoemulsion treatments, including CNE, CrBL-EONE, and D-LNE, after eight weeks of storage at 5 °C. There was no visually noticeable separation of the organic phase from the aqueous phase during the first three weeks, except for the CNE treatment, where the separation was exceedingly slight. Phase separation between the organic and aqueous phases started for all the treatments from the fourth week, although it was not significant as the CI% was 0.2, 0.1, and 0.1 for CNE, CrBL-EONE, and D-LNE, respectively. The CI% values remained almost stable during the fourth and fifth weeks. The values of the CI% increased from 0.4 to 0.6 and then 1.4 during the sixth, seventh, and eighth weeks, respectively.

On the other hand, the increase in the CI% was significantly lower compared with the CrBL-EONE and D-LNE treatments, which showed the same performance during the same storage time with the values of 0.2, 0.3, and 0.3, respectively. In general, the performance of the three treatments was acceptable and stable during the storage period, which lasted eight weeks at 5 °C. However, the CrBL-EONE and D-LNE treatments showed better performance and stability than the CNE treatment. Previous studies indicated several factors that may affect physicochemical properties, including the physical stability of essential oil nanoemulsions during storage. Such factors as nanoemulsion ingredients and preparation methods directly affect the values of particle size (*Z*-average), polydispersity index (PDI), and the droplets' hydrostatic potential (ζ-potential) [48]. Particularly, the optimal values of ζ-potential (–20) are among the significant parameters that indicate the physical stability of nanoemulsions. Higher values of ζ-potential (negative or positive) lead to an increase in repulsive forces at the expense of attractive forces, which in turn leads to a decrease in the coalescence and creaming index values of nanoemulsion droplets [49], thus increasing the physical stability. The method of preparing the nanoemulsion that was applied to all the treatments under study based on high-speed homogenization followed by pulsed sonication and high-pressure homogenizer processes along with the effect of

Tween-80 as a nonionic surfactant effectively contributed to achieving the optimal values of ζ-potential, which enhanced the physical stability of each of the three nanoemulsion treatments (Figure 2).

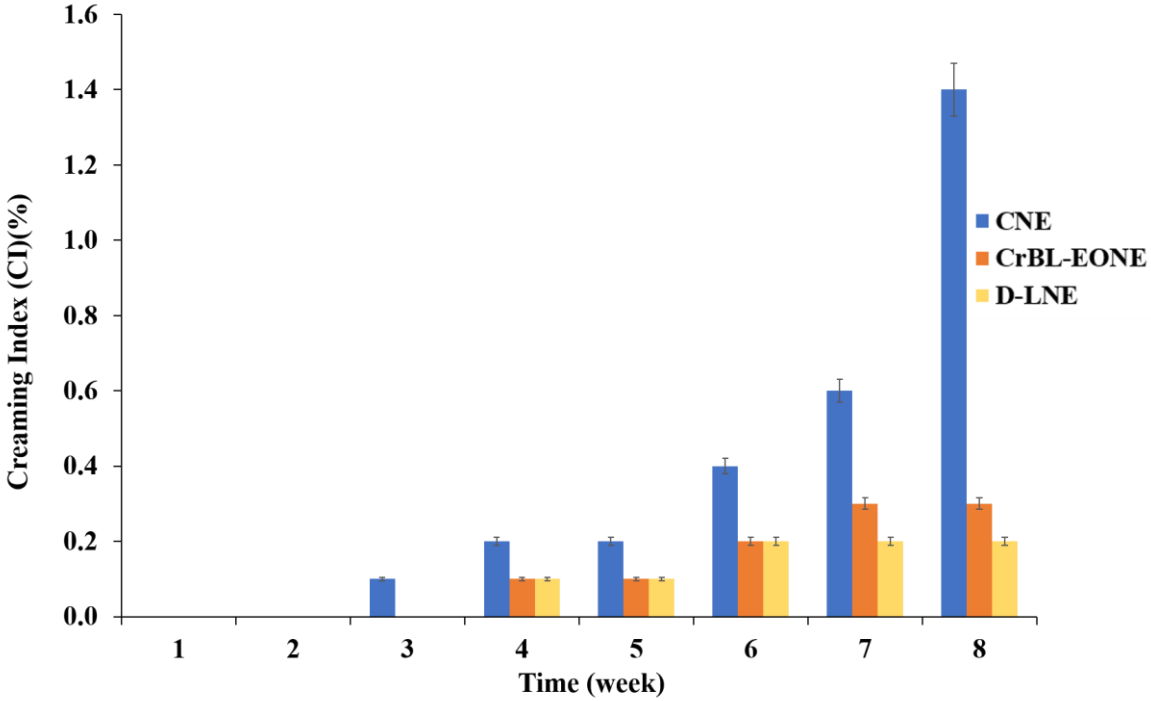

Figure 3. The creaming index (CI%) values of the control nanoemulsion treatment (CNE), *C. reticulata* leaf essential oil nanoemulsion (CrBL-EONE), and D-limonene nanoemulsion (D-LNE) after eight weeks of storage at 5 °C.

3.7. Microscopy CLSM Observation

Morphological observations using CLSM showed that the produced nanoemulsion droplets possessed a spherical and symmetrical shape, as shown in Figure 4a–c. The CLSM observations showed that OSA-MS efficiently coated the organic phase of CrBL-EO carried by almond oil. Among the CLSM observations, it was shown that CrBL-EONE (Figure 4b) and D-LNE (Figure 4c) had an advantage in terms of particle size, shape, and thickness compared with the control treatment (Figure 4a). The organic phase was incorporated into nanoemulsion formulation systems, and a nanoemulsion with spherical morphology was produced.

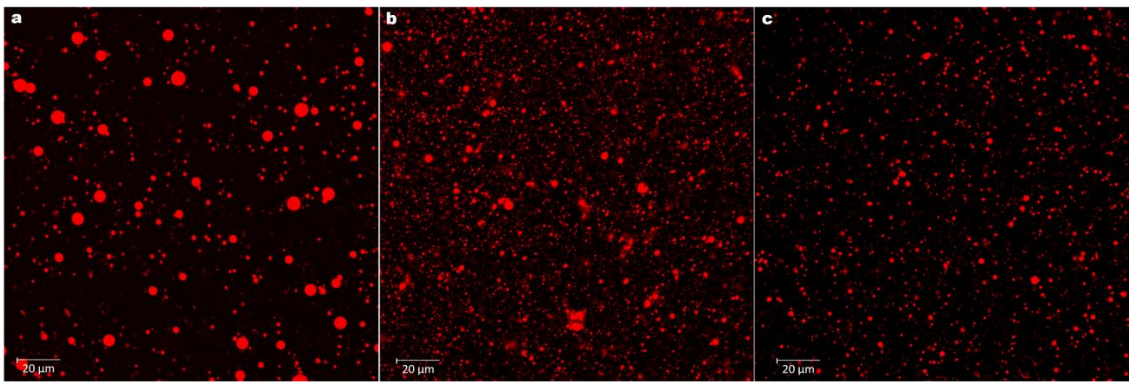

Figure 4. CLSM observations of (**a**) the control nanoemulsion (CNE) treatment, (**b**) *C. reticulata* leaf essential oil nanoemulsion (CrBL-EONE) treatment, and (**c**) D-limonene nanoemulsion (D-LNE) treatment.

Similar findings were reported by Wang et al. [50] who studied the effect of OSA-MS on the physicochemical characteristics of mint flavor nanoemulsion.

3.8. Thermal Autoxidation and Stability Measurement

Figure 5 shows the IA% values of the CrBL-EO_{EUS2}, CrBL-EONE, D-LNE, TBHQ, and D-Limonene treatments in the coupled system of *β*-CLE with the incubation time of 20, 40, and 60 min at 50 °C. The IA% values at the final incubation time (60 min) decreased dose-dependently in the following order: TBHQ (95.95%), D-LNE (95.1%), D-limonene (94.38%), CrBL-EO_{EUS2} (87.12%), and CrBL-EONE (86.43%).

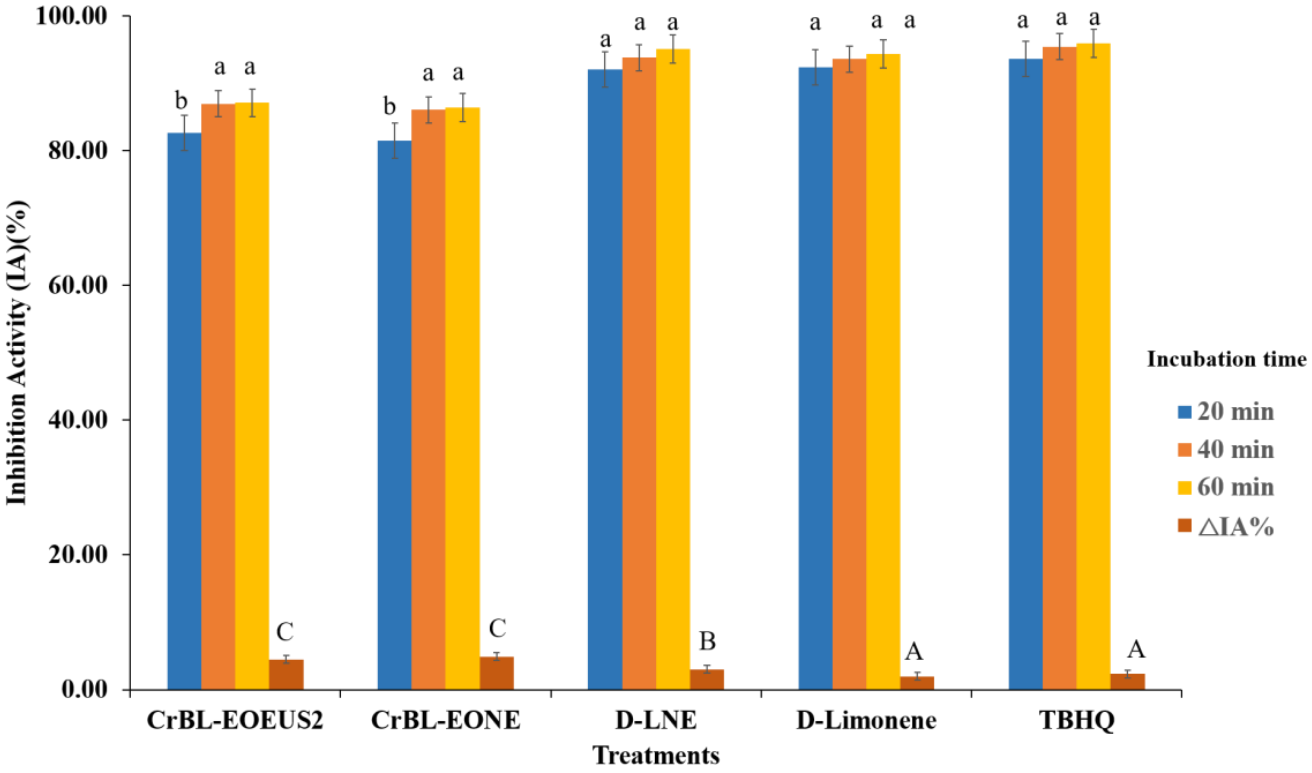

Figure 5. Inhibition activity (IA%) of the essential oil of *C. reticulata* with pre-enzymolysis and ultrasound–microwave treatment (CrBL-EO_{EUS2}), *C. reticulata* essential oil nanoemulsion (CrBL-EONE), D-limonene nanoemulsion (D-LNE), D-limonene, and TBHQ in the *β*-carotene color in the coupled system (*β*-CLE). Bars bearing the same lowercase letters indicate no significant differences in the treatments during a unit of time (20, 40, 60 min). In comparison, bars bearing the same capital letters indicate no significant differences in the ΔIA% between the treatments.

The bleaching rate of the coupled *β*-CLE system was measured using the colorimetric method based on the optical density (470 nm) during 60 min of the total incubation time (Figure 6). The bleaching rate curves show a decrease in the optical density (470 nm) values in the presence of CrBL-EO_{EUS2}, CrBL-EONE, D-LNE, D-Limonene, and TBHQ of the coupled system of *β*-CLE. The curves in Figure 6 show that the control treatment was less resistant and efficient in maintaining the color of *β*-carotene in the coupled system of *β*-CLE.

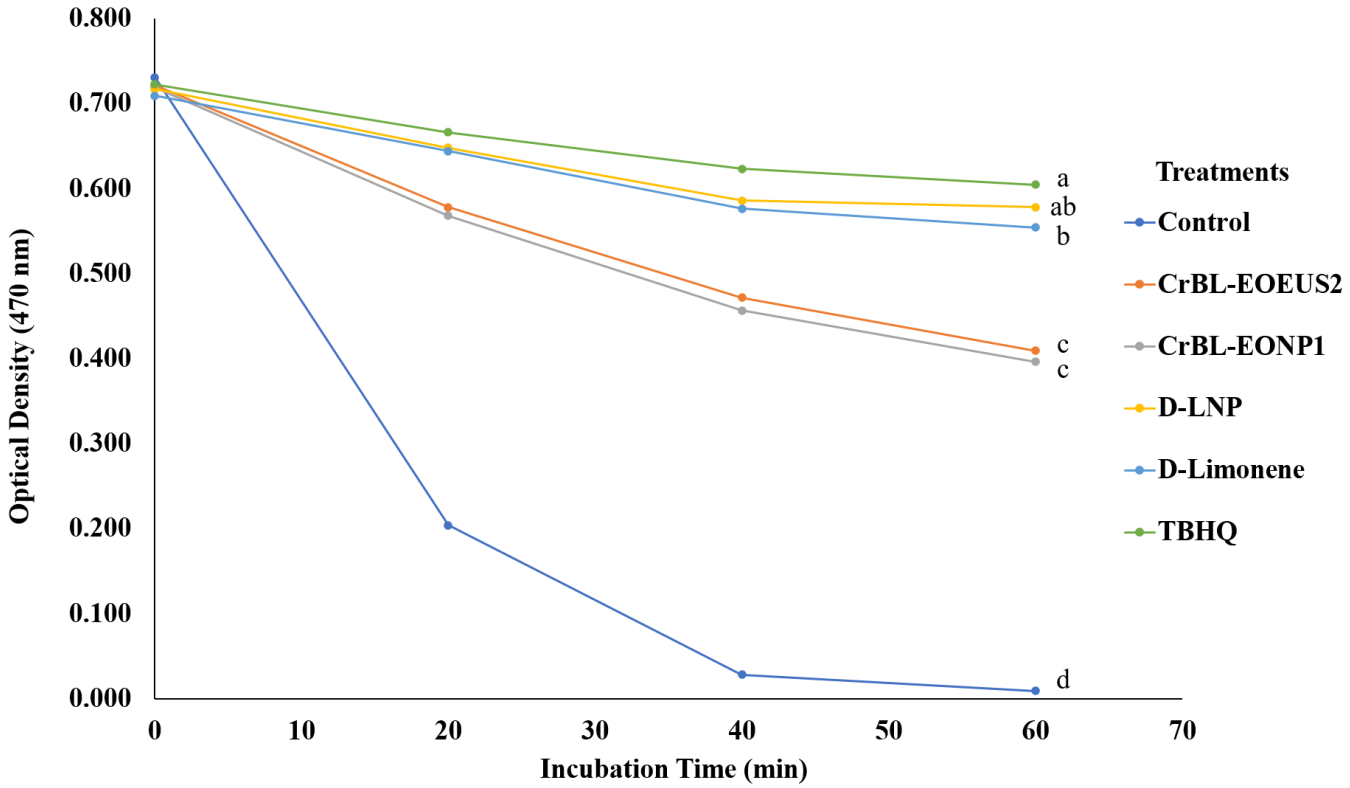

Figure 6. The bleaching rate curves (at an optical density of 470 nm) of the *β*-carotene color in the coupled system of *β*-CLE in the presence of the essential oil of *C. reticulata* with pre-enzymolysis and ultrasound–microwave treatment (CrBL-EO_{EUS2}), *C. reticulata* essential oil nanoemulsion (CrBL-EONE), D-limonene nanoemulsion (D-LNE), D-limonene, and TBHQ. Lines with the same lowercase letters indicate no significant differences in treatment at the final incubation time (60 min).

In contrast, the TBHQ treatment followed by the D-LNE and D-limonene treatments featured the highest resistance to thermal oxidation at 50 °C and degradation conditions among all the treatments, and thus the highest ability to protect the color of *β*-carotene in the *β*-CLE system, with no statistically significant differences between them. At the same time, both the CrBL-EO_{EUS2} and CrBL-EONE treatments showed a high ability to maintain the color of *β*-carotene and protect the *β*-CLE system from oxidation, with no significant differences in the optical density (470 nm) values between the two treatments (CrBL-EO_{EUS2} and CrBL-EONE).

Table 4 shows the DR (between 0 and 60 min, at 50 °C) and the R^2 values (between 0 to 60 min) of the *β*-CLE coupled system in the presence of the CrBL-EO_{EUS2}, CrBL-EONE, D-LNE, D-limonene, TBHQ, and control treatments.

The lower the DR, the higher the efficiency of maintaining the *β*-CLE coupled system from deterioration and oxidation. The DR at the final incubation time (60 min) along with the R^2 values of the TBHQ, D-LNE, D-limonene, CrBL-EO_{EUS2}, CrBL-EONE, and control treatments were as follows: 0.003 (R^2 = 0.9526), 0.0036 (R^2 = 0.8280), 0.0041 (R^2 = 0.9300), 0.0094 (R^2 = 0.9895), 0.0099 (R^2 = 0.9856), and 0.0544 (R^2 = 0.7500), respectively. Compared with the control treatment, the TBHQ, D-limonene, CrBL-EO_{EUS2}, and CrBL-EONE treatments showed high resistance against oxidation processes.

By comparing the results in Figures 5 and 6 and Table 4, it can be concluded that the TBHQ treatment had the highest long-term stability and IA% and the lowest DR (during 60 min at 50 °C) against the oxidation process, followed by the D-LNE, D-limonene, CrBL-EO_{EUS2}, and CrBL-EONE treatments. In addition, *β*-CLE has a higher ability to resist oxidative deterioration and maintains the color of *β*-carotene sequentially from degradation when the chemical composition of the sample added can donate hydrogen

ions (H^+) or prevent the reaction of reactive oxygen species such as peroxides (ROOR), hydroxyl radical ($HO^\bullet$), superoxide (O_2^-), singlet oxygen (O=O), or α-O [51]. The added sample donates hydrogen ions to prevent or delay the oxidation process in β-CLE. The inhibition activity (IA%) of CrBL-EO_{EUS2} D-LNE, and CrBL-EONE can be attributed to their chemical composition rich in chemical compounds that donate free hydrogen ions H^+.

Table 4. The degradation rate (DR) and the R^2 values of the β-CLE coupled system in the presence of pre-enzymolysis and ultrasound–microwave treatment (CrBL-EO_{EUS2}), *C. reticulata* leaf essential oil nanoemulsion (CrBL-EONE), D-limonene nanoemulsion (D-LNE), D-limonene, TBHQ, and control treatments between 0 min and the final incubation time (60 min) at 50 °C.

Treatment System	DR				
	0 min	20 min	40 min	60 min	R^2
Control	0	0.0213 ^{c,A}	0.0544 ^{c,B}	0.00544 ^{c,B}	0.7500
CrBL-EO_{EUS2}	0	0.0037 ^{b,A}	0.0071 ^{b,B}	0.0094 ^{b,B}	0.9895
CrBL-EONE	0	0.0039 ^{b,A}	0.0076 ^{b,B}	0.0099 ^{b,C}	0.9856
D-LNE	0	0.0017 ^{a,A}	0.0034 ^{a,B}	0.0036 ^{a,B}	0.8280
D-limonene	0	0.0016 ^{a,A}	0.0035 ^{a,B}	0.0041 ^{a,B}	0.9300
TBHQ	0	0.0014 ^{a,A}	0.0025 ^{a,B}	0.0030 ^{a,B}	0.9526

The values were expressed as the means ± SD (n = 3). Small superscripts (in columns) indicate statistical significance between the treatments, while capital superscripts (in rows) indicate statistical significance between the incubation times. Treatments with the means followed by the same superscripts do not differ significantly ($p < 0.05$).

4. Conclusions

In conclusion, it can be stated that cellulose and hemicellulase can hydrolyze plant cell walls, enhancing the efficiency of the essential oil isolated from the leaves of *Citrus reticulata* Blanco (tangerine). All the treatments of *C. reticulata* essential oil showed high potential in terms of the free radical scavenging activity. There was a synergistic effect between the enzymatic treatment using a mixture of cellulase/hemicellulase and the ultrasound–microwave integrated treatment. There was an integral effect between amorphous OSA-MS and almond oil in enhancing the efficiency of the bioactive *C. reticulata* essential oil nanoemulsion. The selected components of the produced nanoemulsion matrix contributed to the achievement of the desired values for each *Z*-average, PDI, and ζ-potential. The essential oil of *C. reticulata* and the formulated nanoemulsion of *C. reticulata* leaf essential oil had the optimal values of anti-free radical activity based on the DPPH and ABTS assays. In addition, they also had the highest lipid maintenance capacity of linoleic acid and β-carotene against oxidative degradation. OSA-MS showed excellent characteristics as a wall material in preparing *C. reticulata* leaf essential oil nanoemulsions due to its distinctive chemical composition consisting of an amphipathic molecule with hydrophobic and hydrophilic groups. Almond oil was also shown to be effective as a carrier material in protecting *C. reticulata* leaf essential oil. The current findings open up promising avenues for potential uses of *C. reticulata* leaf nanoemulsion as an additive in food products as a safe alternative to synthetic additives.

Author Contributions: Conceptualization, M.M.A.R. and A.D.S.G.; data curation, A.D.S.G. and Y.D.; formal analysis, M.M.A.R.; funding acquisition, M.M.A.R. and L.Y.; investigation, M.M.A.R.; methodology, M.M.A.R.; project administration, L.Y.; resources, L.Y.; software, M.M.A.R., A.D.S.G. and Y.D.; supervision, M.M.A.R.; validation, L.Y.; visualization, M.M.A.R.; writing—original draft preparation, M.M.A.R.; writing—review and editing, A.D.S.G. All authors have read and agreed to the published version of the manuscript.

Funding: This research was fully funded by a grant from Yibin University (412-0218017302) and partially funded by the Solid-State Fermentation Resource Utilization Key Laboratory of the Sichuan Province (2020GTJ005 and 2020GTY004).

Institutional Review Board Statement: Not applicable.

Informed Consent Statement: Not applicable.

Data Availability Statement: Data is contained within the article.

Conflicts of Interest: The authors declare no conflict of interest.

References

1. Reis, D.R.; Ambrosi, A.; Di Luccio, M. Encapsulated essential oils: A perspective in food preservation. *Futur. Foods* **2022**, *5*, 100126. [CrossRef]
2. Rashed, M.M.; Ghaleb, A.D.; Li, J.; Al-Hashedi, S.A.; Rehman, A. Functional-characteristics of Zanthoxylum schinifolium (Siebold & Zucc.) essential oil nanoparticles. *Ind. Crop. Prod.* **2020**, *161*, 113192. [CrossRef]
3. Rashed, M.M.; Tong, Q.; Abdelhai, M.H.; Gasmalla, M.A.; Ndayishimiye, J.B.; Chen, L.; Ren, F. Effect of ultrasonic treatment on total phenolic extraction from Lavandula pubescens and its application in palm olein oil industry. *Ultrason. Sonochem.* **2016**, *29*, 39–47. [CrossRef] [PubMed]
4. Morais, M.G.; Saldanha, A.A.; Azevedo, L.S.; Mendes, I.C.; Rodrigues, J.P.C.; Amado, P.A.; Farias, K.D.S.; Zanuncio, V.S.S.; Cassemiro, N.S.; da Silva, D.B.; et al. Antioxidant and anti-inflammatory effects of fractions from ripe fruits of Solanum lycocarpum St. Hil. (Solanaceae) and putative identification of bioactive compounds by GC–MS and LC-DAD-MS. *Food Res. Int.* **2022**, *156*, 111145. [CrossRef] [PubMed]
5. Gonfa, T.; Fisseha, A.; Thangamani, A. Isolation, characterization and drug-likeness analysis of bioactive compounds from stem bark of Warburgia ugandensis Sprague. *Chem. Data Collect.* **2020**, *29*, 100535. [CrossRef]
6. Al-Ali, R.M.; Al-Hilifi, S.A.; Rashed, M.M. Fabrication, characterization, and anti-free radical performance of edible packaging-chitosan film synthesized from shrimp shell incorporated with ginger essential oil. *J. Food Meas. Charact.* **2021**, *15*, 2951–2962. [CrossRef]
7. Alasalvar, H.; Yildirim, Z. Ultrasound-assisted extraction of antioxidant phenolic compounds from Lavandula angustifolia flowers using natural deep eutectic solvents: An experimental design approach. *Sustain. Chem. Pharm.* **2021**, *22*, 100492. [CrossRef]
8. da Silva, B.D.; Rosário, D.K.A.D.; Weitz, D.A.; Conte-Junior, C.A. Essential oil nanoemulsions: Properties, development, and application in meat and meat products. *Trends Food Sci. Technol.* **2022**, *121*, 1–13. [CrossRef]
9. Angane, M.; Swift, S.; Huang, K.; Butts, C.A.; Quek, S.Y. Essential Oils and Their Major Components: An Updated Review on Antimicrobial Activities, Mechanism of Action and Their Potential Application in the Food Industry. *Foods* **2022**, *11*, 464. [CrossRef] [PubMed]
10. Wang, Y.; Du, Y.-T.; Xue, W.-Y.; Wang, L.; Li, R.; Jiang, Z.-T.; Tang, S.-H.; Tan, J. Enhanced preservation effects of clove (Syzygium aromaticum) essential oil on the processing of Chinese bacon (preserved meat products) by beta cyclodextrin metal organic frameworks (β-CD-MOFs). *Meat Sci.* **2023**, *195*, 108998. [CrossRef]
11. Das, S.; Gazdag, Z.; Szente, L.; Meggyes, M.; Horváth, G.; Lemli, B.; Kunsági-Máté, S.; Kuzma, M.; Kőszegi, T. Antioxidant and antimicrobial properties of randomly methylated β cyclodextrin–captured essential oils. *Food Chem.* **2019**, *278*, 305–313. [CrossRef] [PubMed]
12. Partheniadis, I.; Stathakis, G.; Tsalavouti, D.; Heinämäki, J.; Nikolakakis, I. Essential Oil—Loaded Nanofibers for Pharmaceutical and Biomedical Applications: A Systematic Mini-Review. *Pharmaceutics* **2022**, *14*, 1799. [CrossRef]
13. Moreira, P.; Sousa, F.J.; Matos, P.; Brites, G.S.; Gonçalves, M.J.; Cavaleiro, C.; Figueirinha, A.; Salgueiro, L.; Batista, M.T.; Branco, P.C.; et al. Chemical Composition and Effect against Skin Alterations of Bioactive Extracts Obtained by the Hydrodistillation of Eucalyptus globulus Leaves. *Pharmaceutics* **2022**, *14*, 561. [CrossRef] [PubMed]
14. Graf, M.; Stappen, I. Beyond the Bark: An Overview of the Chemistry and Biological Activities of Selected Bark Essential Oils. *Molecules* **2022**, *27*, 7295. [CrossRef] [PubMed]
15. Ullah, H.; Wilfred, C.D.; Shaharun, M.S. Comparative assessment of various extraction approaches for the isolation of essential oil from polygonum minus using ionic liquids. *J. King Saud Univ. Sci.* **2019**, *31*, 230–239. [CrossRef]
16. El Zerey-Belaskri, A.; Belyagoubi-Benhammou, N.; Benhassaini, H. From Traditional Knowledge to Modern Formulation: Potential and Prospects of Pistacia atlantica Desf. Essential and Fixed Oils Uses in Cosmetics. *Cosmetics* **2022**, *9*, 109. [CrossRef]
17. Boiangiu, R.S.; Bagci, E.; Dumitru, G.; Hritcu, L.; Todirascu-Ciornea, E. Angelica purpurascens (Avé-Lall.) Gilli. Essential Oil Improved Brain Function via Cholinergic Modulation and Antioxidant Effects in the Scopolamine-Induced Zebrafish (Danio rerio) Model. *Plants* **2022**, *11*, 1096. [CrossRef] [PubMed]
18. Yeom, J.; Shim, W.S.; Kang, N.G. Eco-Friendly Silica Microcapsules with Improved Fragrance Retention. *Appl. Sci.* **2022**, *12*, 6759. [CrossRef]
19. Prommaban, A.; Chaiyana, W. Microemulsion of essential oils from citrus peels and leaves with anti-aging, whitening, and irritation reducing capacity. *J. Drug Deliv. Sci. Technol.* **2022**, *69*, 103188. [CrossRef]
20. Sharma, S.; Barkauskaite, S.; Jaiswal, A.K.; Jaiswal, S. Essential oils as additives in active food packaging. *Food Chem.* **2021**, *343*, 128403. [CrossRef]
21. Shorbagi, M.; Fayek, N.M.; Shao, P.; Farag, M.A. Citrus reticulata Blanco (the common mandarin) fruit: An updated review of its bioactive, extraction types, food quality, therapeutic merits, and bio-waste valorization practices to maximize its economic value. *Food Biosci.* **2022**, *47*, 101699. [CrossRef]
22. Singh, B.; Singh, J.P.; Kaur, A.; Yadav, M.P. Insights into the chemical composition and bioactivities of citrus peel essential oils. *Food Res. Int.* **2021**, *143*, 110231. [CrossRef]

23. Rashed, M.M.; Tong, Q.; Nagi, A.; Li, J.; Khan, N.U.; Chen, L.; Rotail, A.; Bakry, A.M. Isolation of essential oil from Lavandula angustifolia by using ultrasonic-microwave assisted method preceded by enzymolysis treatment, and assessment of its biological activities. *Ind. Crop. Prod.* **2017**, *100*, 236–245. [CrossRef]
24. Pongsumpun, P.; Iwamoto, S.; Siripatrawan, U. Response surface methodology for optimization of cinnamon essential oil nanoemulsion with improved stability and antifungal activity. *Ultrason. Sonochem.* **2020**, *60*, 104604. [CrossRef] [PubMed]
25. Xiao, Z.; Kang, Y.; Hou, W.; Niu, Y.; Kou, X. Microcapsules based on octenyl succinic anhydride (OSA)-modified starch and maltodextrins changing the composition and release property of rose essential oil. *Int. J. Biol. Macromol.* **2019**, *137*, 132–138. [CrossRef]
26. Sharma, S.; Loach, N.; Gupta, S.; Mohan, L. Evaluation of larval toxicity, mode of action and chemical composition of citrus essential oils against Anopheles stephensi and Culex quinquefasciatus. *Biocatal. Agric. Biotechnol.* **2022**, *39*, 102284. [CrossRef]
27. Rashed, M.M.; Mahdi, A.A.; Ghaleb, A.D.; Zhang, F.R.; YongHua, D.; Qin, W.; WanHai, Z. Synergistic effects of amorphous OSA-modified starch, unsaturated lipid-carrier, and sonocavitation treatment in fabricating of Lavandula angustifolia essential oil nanoparticles. *Int. J. Biol. Macromol.* **2020**, *151*, 702–712. [CrossRef] [PubMed]
28. British Pharmacopoeia Commission; Great Britain. Medicines Commission. In *British Pharmacopoeia 2000*; Bernan Press (PA): Blue Ridge Summit, PA, USA, 2000; Volume 1.
29. Rashed, M.M.A.; Ghaleb, A.D.S.; Li, J.; Nagi, A.; Hua-Wei, Y.; Wen-You, Z.; Tong, Q. Enhancement of Mass Transfer Intensification for Essential Oil Release from Lavandula pubescence Using Integrated Ultrasonic-Microwave Technique and Enzymatic Pretreatment. *ACS Sustain. Chem. Eng.* **2018**, *6*, 1639–1649. [CrossRef]
30. Rashed, M.M.; Zhang, C.; Ghaleb, A.D.; Li, J.; Nagi, A.; Majeed, H.; Bakry, A.M.; Haider, J.; Xu, Z.; Tong, Q. Techno-functional properties and sustainable application of nanoparticles-based Lavandula angustifolia essential oil fabricated using unsaturated lipid-carrier and biodegradable wall material. *Ind. Crop. Prod.* **2019**, *136*, 66–76. [CrossRef]
31. Liu, M.; Pan, Y.; Feng, M.; Guo, W.; Fan, X.; Feng, L.; Huang, J.; Cao, Y. Garlic essential oil in water nanoemulsion prepared by high-power ultrasound: Properties, stability and its antibacterial mechanism against MRSA isolated from pork. *Ultrason. Sonochem.* **2022**, *90*, 106201. [CrossRef]
32. Mkaddem, M.G.; Zrig, A.; Ben Abdallah, M.; Romdhane, M.; Okla, M.K.; Al-Hashimi, A.; Alwase, Y.A.; Hegab, M.Y.; Madany, M.M.Y.; Hassan, A.H.A.; et al. Variation of the Chemical Composition of Essential Oils and Total Phenols Content in Natural Populations of *Marrubium vulgare* L. *Plants* **2022**, *11*, 612. [CrossRef]
33. Pakdel, H.; Pantea, D.M.; Roy, C. Production of dl-limonene by vacuum pyrolysis of used tires. *J. Anal. Appl. Pyrolysis* **2001**, *57*, 91–107. [CrossRef]
34. Visakh, N.U.; Pathrose, B.; Chellappan, M.; Ranjith, M.; Sindhu, P.; Mathew, D. Chemical characterisation, insecticidal and antioxidant activities of essential oils from four Citrus spp. fruit peel waste. *Food Biosci.* **2022**, *50*, 102163. [CrossRef]
35. Liu, Z.; Li, H.; Cui, G.; Wei, M.; Zou, Z.; Ni, H. Efficient extraction of essential oil from Cinnamomum burmannii leaves using enzymolysis pretreatment and followed by microwave-assisted method. *LWT* **2021**, *147*, 111497. [CrossRef]
36. Wan, N.; Kou, P.; Pang, H.-Y.; Chang, Y.-H.; Cao, L.; Liu, C.; Zhao, C.-J.; Gu, C.-B.; Fu, Y.-J. Enzyme pretreatment combined with ultrasonic-microwave-assisted surfactant for simultaneous extraction of essential oil and flavonoids from Baeckea frutescens. *Ind. Crop. Prod.* **2021**, *174*, 114173. [CrossRef]
37. Chen, Y.; Xu, F.; Pang, M.; Jin, X.; Lv, H.; Li, Z.; Lee, M. Microwave-assisted hydrodistillation extraction based on microwave-assisted preparation of deep eutectic solvents coupled with GC-MS for analysis of essential oils from clove buds. *Sustain. Chem. Pharm.* **2022**, *27*, 100695. [CrossRef]
38. Araujo, N.M.P.; Pereira, G.A.; Arruda, H.S.; Prado, L.G.; Ruiz, A.L.T.G.; Eberlin, M.N.; de Castro, R.J.S.; Pastore, G.M. Enzymatic treatment improves the antioxidant and antiproliferative activities of *Adenanthera pavonina* L. seeds. *Biocatal. Agric. Biotechnol.* **2019**, *18*, 101002. [CrossRef]
39. Xiong, L.; Hu, W.-B.; Yang, Z.-W.; Chen, H.; Ning, W.; Xin, L.; Wang, W.-J. Enzymolysis-ultrasonic assisted extraction of flavanoid from Cyclocarya paliurus (Batal) Iljinskaja:HPLC profile, antimicrobial and antioxidant activity. *Ind. Crop. Prod.* **2019**, *130*, 615–626. [CrossRef]
40. Jiao, J.; Li, Z.-G.; Gai, Q.-Y.; Li, X.-J.; Wei, F.-Y.; Fu, Y.-J.; Ma, W. Microwave-assisted aqueous enzymatic extraction of oil from pumpkin seeds and evaluation of its physicochemical properties, fatty acid compositions and antioxidant activities. *Food Chem.* **2014**, *147*, 17–24. [CrossRef] [PubMed]
41. Hou, K.; Bao, M.; Wang, L.; Zhang, H.; Yang, L.; Zhao, H.; Wang, Z. Aqueous enzymatic pretreatment ionic liquid–lithium salt based microwave–assisted extraction of essential oil and procyanidins from pinecones of Pinus koraiensis. *J. Clean. Prod.* **2019**, *236*, 117581. [CrossRef]
42. Pasias, I.N.; Ntakoulas, D.D.; Raptopoulou, K.; Gardeli, C.; Proestos, C. Chemical Composition of Essential Oils of Aromatic and Medicinal Herbs Cultivated in Greece—Benefits and Drawbacks. *Foods* **2021**, *10*, 2354. [CrossRef]
43. Marathe, S.J.; Jadhav, S.B.; Bankar, S.B.; Dubey, K.K.; Singhal, R.S. Improvements in the extraction of bioactive compounds by enzymes. *Curr. Opin. Food Sci.* **2019**, *25*, 62–72. [CrossRef]
44. Mohammadpour, H.; Sadrameli, S.M.; Eslami, F.; Asoodeh, A. Optimization of ultrasound-assisted extraction of Moringa peregrina oil with response surface methodology and comparison with Soxhlet method. *Ind. Crop. Prod.* **2019**, *131*, 106–116. [CrossRef]

45. Hou, K.; Yang, X.; Bao, M.; Chen, F.; Tian, H.; Yang, L. Composition, characteristics and antioxidant activities of fruit oils from Idesia polycarpa using homogenate-circulating ultrasound-assisted aqueous enzymatic extraction. *Ind. Crop. Prod.* **2018**, *117*, 205–215. [CrossRef]
46. Floegel, A.; Kim, D.-O.; Chung, S.-J.; Koo, S.I.; Chun, O.K. Comparison of ABTS/DPPH assays to measure antioxidant capacity in popular antioxidant-rich US foods. *J. Food Compos. Anal.* **2011**, *24*, 1043–1048. [CrossRef]
47. Zhang, B.; Zheng, L.; Liang, S.; Lu, Y.; Zheng, J.; Zhang, G.; Li, W.; Jiang, H. Encapsulation of Capsaicin in Whey Protein and OSA-Modified Starch Using Spray-Drying: Physicochemical Properties and Its Stability. *Foods* **2022**, *11*, 612. [CrossRef] [PubMed]
48. Ozogul, Y.; Karsli, G.T.; Durmuş, M.; Yazgan, H.; Oztop, H.M.; McClements, D.J.; Ozogul, F. Recent developments in industrial applications of nanoemulsions. *Adv. Colloid Interface Sci.* **2022**, *304*, 102685. [CrossRef]
49. Marhamati, M.; Ranjbar, G.; Rezaie, M. Effects of emulsifiers on the physicochemical stability of Oil-in-water Nanoemulsions: A critical review. *J. Mol. Liq.* **2021**, *340*, 117218. [CrossRef]
50. Wang, K.; Cheng, L.; Li, Z.; Li, C.; Hong, Y.; Gu, Z. The degree of substitution of OSA-modified starch affects the retention and release of encapsulated mint flavour. *Carbohydr. Polym.* **2022**, *294*, 119781. [CrossRef] [PubMed]
51. Bolduc, J.A.; Collins, J.A.; Loeser, R.F. Reactive oxygen species, aging and articular cartilage homeostasis. *Free Radic. Biol. Med.* **2019**, *132*, 73–82. [CrossRef]